September 1985 LRP 276/85

MHD STABILITY OF TOROIDAL CONFINEMENT

F. Troyon

Lecture presented at the

Course and Workshop
Basic Physical Processes of Toroidal Fusion Plasmas

Varenna, Italy, August 26 - September 3, 1985

MHD STABILITY OF TOROIDAL CONFINEMENT

F. Troyon

Centre de Recherches en Physique des Plasmas
Association Euratom - Confédération Suisse
Ecole Polytechnique Fédérale de Lausanne
21, Av. des Bains, CH-1007 Lausanne/Switzerland

ABSTRACT

Ideal MHD instabilities grow on a fast time scale given by the Alfvén wave transit time across the major radius, usually in the microsecond range. These instabilities are driven by the current and the pressure. In Tokamaks they lead to a current limitation and a pressure limit. The main results of the standard large aspect circular cross-section Tokamak theory are presented (internal and external kinks). The effect of toricity is then demonstrated with some numerical results. The most important new element is the appearance of ballooning of modes across magnetic surface and pressure destabilisation of the long wavelength external kinks. A semi-empirical scaling law which gives the maximum pressure which can be confined in a Tokamak is presented with the supporting experimental status.

1. INTRODUCTION

The range of operation of most toroidal plasma confinement devices is limited by instabilities. The most dangerous instabilities are macroscopic and describable by the magnetohydrodynamic model (MHD). The characteristic time scale for the fastest of these instabilities is the Alfvén transit time

across the major radius of the plasma R

$$\tau_o = \frac{R\sqrt{\rho_o \mu_o}}{B_\phi} \quad \text{(MKS units)} \qquad (1)$$

This is in the submicrosecond range for typical tokamak equilibria, so fast that the magnetic field is frozen in the plasma as it moves. This is describable by ideal MHD. When there are no such instabilities on this time scale, there can still be slower growing instabilities due to the breaking up of the magnetic field topology on some surfaces. These are the resistive instabilities.

Ideal MHD instabilities are feared because in the past they have been the cause of the failure of many confinement schemes and because they could limit the performance of tokamaks. Resistive instabilities can saturate so that their existence is not in itself a lethal default for a confinement system even though in their nonlinear stage they may lead to catastrophic operational limits.

This lecture is devoted to the ideal MHD stability properties of tokamaks only. To illustrate the argumentation ample use is made of results obtained in Lausanne because they are readily available to us. In many instances, results of other groups could equally well serve the argument.

It may be surprising that after 30 years of intense work in this domain one does not have yet a fully coherent picture of the ideal MHD stability of as simple a structure as a tokamak. Much of our present understanding is based on partial and disconnected bits of information which we tend to consider as proved because we are used to hear about it.

2. DESCRIPTION OF THE EQUILIBRIUM

A tokamak equilibrium is characterized by the shape of its surface S, the vacuum toroidal field B_ϕ, the total toroidal current I, the volume average pressue $\langle p \rangle$. These are global, external parameters. To fully specify the equilibrium, we need to know the pressure profile and the current density profile, or two other equivalent source functions.

Designating by $\psi(r,z)$ the usual poloidal magnetic flux function and by $T(\psi)$ the poloidal current flux function, the magnetic field and the toroidal current density are given by

$$\underline{B} = \frac{T}{r}\,\underline{\hat{e}}_\phi + \frac{1}{r}\,\underline{\nabla}\psi \times \underline{\hat{e}}_\phi, \quad J_\phi = -\frac{T}{r}\frac{dT}{d\psi} - \mu_o r \frac{dp}{d\psi} \qquad (2)$$

The flux function $\psi(r,z)$ satisfies the GSS equation (1)

$$\Delta^*\psi = J_\phi \tag{3}$$

To specify the equilibrium, we can use either the pair of functions $p(\psi)$ and $T(dT/d\psi)$, or $p(\psi)$ and $q(\psi)$, the safety factor defined by

$$q(\psi) = \frac{T}{2\pi} \oint \frac{d\ell}{r^2 B_p} \quad , \tag{4}$$

or $p(\psi)$ and the surface average toroidal current density $dI/d\psi$ defined by

$$\frac{dI}{d\psi} = \frac{d}{d\psi} \iint J_\phi dS = \oint \frac{J_\phi d\ell}{r B_p} \quad . \tag{5}$$

The surface integral in (5) is over a meridian cross-section limited by the magnetic surface ψ. The line integrals in (4) and (5) are along a poloidal field line on the ψ surface. The first two choices are very common. We have found the last choice very convenient.

By substituting (2) into (5), J_ϕ can be expressed directly in terms of $dI/d\psi$ and $dp/d\psi$.

$$J_\phi = - \frac{\frac{dI}{d\psi} + \mu_o \frac{dp}{d\psi} \left\{ r^2 \oint \frac{d\ell}{r^2 B_p} - \oint \frac{d\ell}{B_p} \right\}}{r^2 \oint \frac{d\ell}{r^2 B_p}} \tag{6}$$

We need some more definitions: the volume average β and the poloidal β_I, defined as

$$\beta = \frac{2\mu_o \int p dV}{\int B^2 dV} \quad ; \quad \beta_I = \frac{8\pi \int p dS}{\mu_o I^2} \tag{7}$$

3. THE STABILITY CRITERION

The change in potential energy δW arising from a perturbation of the plasma around its equilibrium position is given by /1/

$$\delta W = \frac{1}{2} \int_{\text{plasma}} d^3x \left\{ \frac{1}{\mu_o} \left| \underline{\delta B} + \mu_o \xi_n (\underline{J}_o \times \hat{\underline{n}}) \right|^2 + \gamma p_o \left| \underline{\nabla} \cdot \underline{\xi} \right|^2 \right.$$
$$\left. - 2\, \underline{J}_o \times \hat{\underline{n}} \cdot \left[(\underline{B}_o \cdot \underline{\nabla}) \hat{\underline{n}} \right] \xi_n^2 \right\} + \frac{1}{2} \int_{\text{vacuum}} d^3x \, \frac{\left| \underline{\nabla} \times \delta \underline{A} \right|^2}{\mu_o} \, . \tag{8}$$

The index o refers to the equilibrium quantities. In the plasma

$\underline{\delta B} = \underline{\nabla} \times (\underline{\xi} \times \underline{B}_o)$, where $\underline{\xi}$ is the displacement from the equilibrium position. The unit vector $\hat{\underline{n}}$ is normal to the magnetic surface: $\hat{\underline{n}} \equiv \underline{\nabla}\psi / |\underline{\nabla}\psi|$. $\delta\underline{A}$ is the perturbation of the vacuum vector potential, with the condition on the plasma surface

$$\hat{\underline{n}} \times \delta\underline{A} = -\xi_n \underline{B}_o \tag{9}$$

If there is a conducting shell which limits the vacuum region one must impose that $\hat{\underline{n}} \times \delta\underline{A} = 0$ on it. Minimizing δW while keeping the norm $\frac{1}{2}\int_{\text{plasma}} d^3x \rho_o |\underline{\xi}|^2$ constant gives the fondamental mode $(\xi, \delta\underline{A})$, and the Rayleigh quotient

$$\omega^2 = \frac{\delta W}{\frac{1}{2}\int d^3x \rho_o |\xi|^2} \tag{10}$$

provides the corresponding eigenfrequency. When $\omega^2 < 0$, the equilibrium is unstable and $|\omega|$ gives the growthrate of the instability. Instability occurs whenever there exists a neighbouring equilibrium with lower potential energy, accessible on the fast time scale ($\delta W < 0$).

This technique is the most appropriate for the systematic study of MHD stability and is implemented in various spectral codes which are of general use now: PEST /2/, ERATO /3/, its variant GATO /4/ and Degtyarev's code /5/. The main advantage over evolution codes is higher accuracy for a given resolution.

4. FOURIER DECOMPOSITION

We make use of the axisymmetry of the tokamak by expanding the deformation in a Fourier series in the toroidal angle ϕ:

$$\begin{pmatrix} \underline{\xi} \\ \delta\underline{A} \end{pmatrix} = \mathcal{R}e \sum_{n=0}^{\infty} \begin{pmatrix} \underline{\xi} \\ \delta\underline{A} \end{pmatrix} e^{in\phi} \tag{11}$$

where on the right of (11) the vectors $\underline{\xi}$ and $\delta\underline{A}$ depend only on ϕ and a poloidal angle. The different ns do not couple in δW so that the minimisation can be done separately for each n, giving each time the fundamental mode for this n. Equation (11) gives explicitely the dependence on ϕ.

We first consider the case $n \neq 0$, since axisymmetric ($n = o$) stability has very different properties.

5. STABILITY OF A PRESSURELESS TOKAMAK

Let us look at the stability of a circular cross-section force-free tokamak ($p = 0$), starting from the standard large aspect ratio theory as

summarized in J. Wesson's review paper /5/.

There remains one global parameter I_p and one profile information I' to fix the equilibirum.

In the large aspect ratio limit $R/a \gg 1$ the magnetic surfaces are circles which can be parametrized with the radius ρ and the polar angle θ. Equilibrium quantities have a weak dependence on θ. After Fourier decomposition of the perturbation in θ, introducing the poloidal mode index m, there is a small coupling between the different ms which can be treated in a perturbative manner.

In the lowest order, equilibrium quantities are independent of θ and each mode has a single m. The safety factor on each surface is related to the average current density $\langle j \rangle = I(\phi)/S(\phi)$ by

$$q = \frac{2B_\phi}{\mu_o R \langle j \rangle} \tag{11}$$

The safety factor at the surface

$$q_a = \frac{2\pi a^2 B_\phi}{\mu_o R I} \tag{12}$$

is used in place of the current I, because it leads to a simpler stability diagram.

At this order, the plasma can be considered as a straight cylinder, with the correspondence $k = n/R$, where k is the axial wavenumber. Higher order terms in $\varepsilon = a/R$ are neglected in δW to remain consistent.

J. Wesson has used this reduced δW to compute the stable operating range for a class of current profiles

$$j_\phi = J_o\left(1 - \frac{r^2}{a^2}\right)^\nu, \tag{13}$$

where $\nu \equiv q_a/q_o - 1$ (q_o is on axis).

The result is shown in Fig. 1. The relevant variables turn out to be q_o and q_a. The stable region is to the left of the line labeled W and above $q_a = 1$, the Kruskal-Shafranov limit. The line W is essentially $q_a/q_o = 2$ with some prongs just below integer values of q_a or just below a low rational number. The most dangerous modes near integer values of q_a have $n = 1$ and $m = q_a$. They are surface kinks and as q_a increases they are more localized near the surface. Below $q_a = 1$ there is a very global and rigid $m = 1$, $n = 1$ kink, growing on the fastest time scale.

For $q_a/q_o < 2$, $(dJ_\phi/d\rho)_a = \infty$, while $(dJ_\phi/d\rho)_a = 0$ for $q_a/q_o > 2$. The W line thus corresponds to the transition to

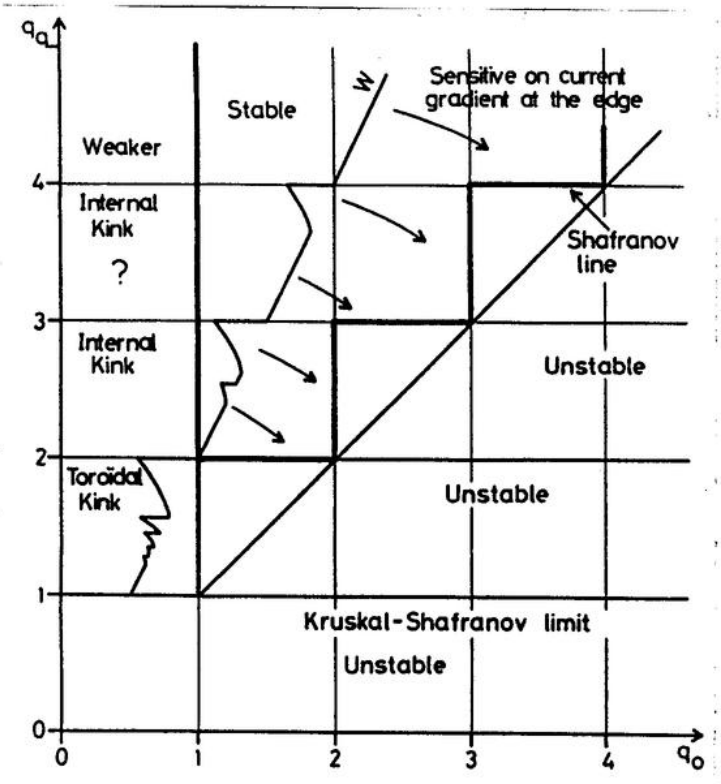

Fig. 1: The ideal MHD stability diagram of a pressureless large aspect ratio circular cross-section tokamak.

$(dJ_\phi/d\rho)_a = 0$, which is necessary to have stability. With a different current profile which has $(dJ_\phi/d\rho)_a = 0$ for any $q_a/q_o > 1$, one can separate the effects of q_a/q_o and of $(dJ_\phi/d\rho)_a \neq 0$. As the current is progressively moved away from the surface (peaked), the W line shifts to the right, showing that the current gradient at the edge is destabilizing. As long as q remains a monotonically increasing function of ρ, the optimum profile (largest stable area) consists of a constant current J_o, which implies a flat $q = q_o$ profile, up to a radius $\rho_b < a$ determined by q_a, and then $J_\phi = 0$ for $\rho_b < \rho \leq a$. V.D. Shafranov /7/ has indeed shown that it improves the stability and reduces the width and size of the prongs. The limit, made of steps along the line $q_a/q_o = 1$, is shown in Fig. 1, labeled as Shafranov line. There is nothing at this order which gives a lower bound on q_o.

6. TOROIDAL EFFECTS

To our knowledge, there has not been a systematic attempt to derive the same stability diagram in toroidal geometry without approximations, using for example spectral codes. We have completed a study which provides some useful information /8/. In order to identify the toroidal effects, the equilibrium is specified by choosing for $dI/d\psi$ the same step function used by Shafranov with the edge rounded off to avoid numerical problems, but nevertheless keeping a current-free region near the surface. The sequence of equilibria with

four different ratios of q_a/q_o is shown in Fig. 3a. The calculation has been done with ERATO and without any conducting shell. Three different aspect ratios have been examined, R/a = 2.5, 5 and 10.

In all cases a n = 1 unstable kink develops when $q_a < 2$, also in the range $q_o < 1$ which is stable in the large aspect ratio theory. An example of such a mode is shown in Fig. 2. It is an F equilibrium with an aspect ratio of 2.5. The mode is a kink with a large shear flow on the q = 1 surface and a strong deformation of the plasma surface. Note that $q_a/q_o = 4.20$.

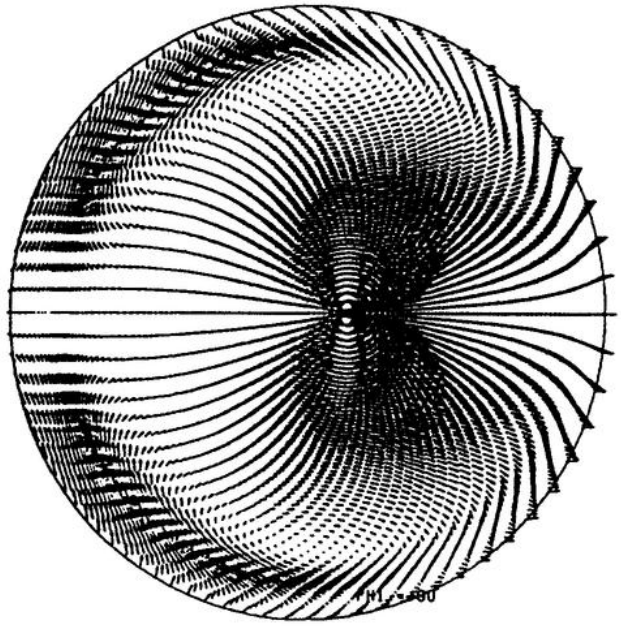

Fig. 2: An unstable n = 1 free-boundary mode in a pressureless, circular cross-section tokamak which has $q_o = 0.34$ and $q_a = 1.44$. The growthrate normalized to τ_o (1) is $|\omega| = 0.183$. The aspect ratio is 2.5 and the current profile is shown in Fig. 3a as F. The major axis is to the left.

Keeping $q_o < 1$ and raising q_a between 2 and 3 the n = 1 mode remains unstable but it becomes weaker growing and more internal. It is not an internal kink since it disappears when a rigid boundary condition is applied at the plasma surface, thus not contradicting the result of M.N. Bussac at al. /10/ which predicts a threshold in p' for this mode. As q_a is increased above 3, the mode still seems to be unstable but the growthrate is in a range where the numerical noise due to the discretisation is such that one cannot make a definite statement. Above $q_a = 4$, the growthrate has definitely lost its significance with the available resolution. The existence of this instability at high values of q_a nevertheless remains an interesting issue to be clarified. These new regions of instability are added in Fig. 1.

In summary, the stable region is limited by $q_o > 1$, $q_a > 2$ and a line which is at best the Shafranov line and which moves to the left when the current is redistributed towards the outer region. An important point is that the n = 1 mode is the most dangerous for the Shafranov current profile but as current is moved towards the edge, higher n modes may become more dangerous at some rational values of q_a. The detailed shape of the stability boundary is thus expected to be sensitive to details of the current profile near the edge but there is a lack of information due to the difficulty of studying short wavelength modes with spectral codes. Reference 9 contains some useful information on this problem but at $\beta \neq 0$.

We have not seen the same stability diagram drawn for a non-circular cross-section tokamak. Numerical stability studies are usually done by moving along constant q_a/q_o lines for purely technical reasons (the equilibirum needs to be computed only once, the change in q being done by changing the toroidal field at the surface) so that drawing such a diagram from published data would require extensive cross-plotting. The information is not sufficient to do this. But from all the cases documented, it appears that the general behaviour remains the same, at least for weakly non-circular plasmas such as JET: If q_a/q_o is too low, bands of instabilities appear just below integer q_a corresponding to crossing the prongs in Fig. 1; if this ratio is too high, as q_o drops below 1 before q_a reaches 2 and since all these calculations have been done with $\beta \neq 0$ and peaked pressure profiles, there appears a n = 1 internal kink when q_o crosses 1; there is an intermediate range of q_a/q_o where stability is achieved down to $q_a \approx 2$. The behaviour in Fig. 1 thus seems to be general. The data in ref. 9 is typical in this respect.

Nevertheless it is clear that for divertor plasmas, where $q_a = \infty$, or for strongly non-circular plasmas, either stronly elongated or indented shapes, the variable q_a looses its meaning and it must be replaced by another expression which has the same dependence on the current. One sometimes uses a definition q_I /11/ which is the q_a of an elliptical plasma having the same elongation and the same constant average current density. But this is one domain where the information is very scanty. More calculations are needed to find the equivalent of the condition $q_a > 2$, namely what is the maximum current which can be carried by a $\beta = 0$ plasma as a function of shape.

7. INSTABILITIES DRIVEN BY PRESSURE ($\beta \neq 0$)

In the large aspect ratio expansion, pressure appears at the same order as toroidal coupling, if one assumes that $\beta_I \sim 1$. It means pressure will start having an influence on stability only if $\beta_I \sim R/a$, the so-called high-β regime. In this regime, one cannot use the straight cylinder approximation, as toroidal effects are crucial. In order to demonstrate these new effects we use again a circular cross-section tokamak with the same flat current profile discussed in the previous section (Fig. 3). The aspect ratio

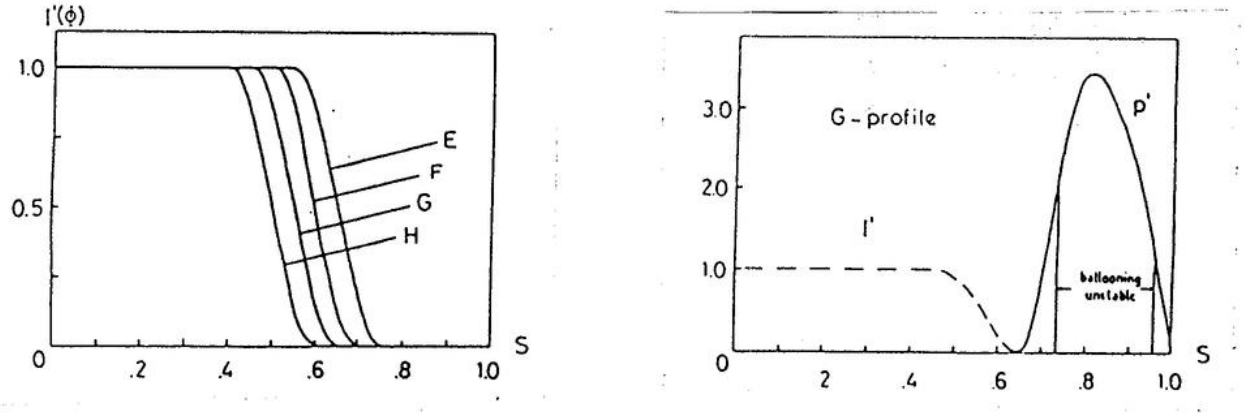

Fig. 3:

a) The shape of the current profile $I' \equiv dI/d\phi$ used in the numerical study of the effect of finite aspect ratio on stability.

b) Shape of $p' \equiv dp/d\phi$ used in the $n = 1$ and $n = \infty$ modes. The value of ϕ where p' starts increasing coincides in the four cases with the value of ϕ where I' falls to zero. For the case G, the ballooning unstable region between 0.73 and 0.95 is also shown. $s \equiv \sqrt{1 - \phi/\phi_{axis.}}$

is fixed at $R/a = 5$. We impose that the total current as well as its profile remains constant $I_N \equiv \mu_o I/aB_\phi = 0{,}5$ as pressure is increased. In the absence of pressure $q_a = 2.6$. For the pressure profile we enforce that it be constant in the region where $I' \neq 0$ and that $p' = 0$ at the surface (Fig. 3b). The plasma is thus made of a hard-core in which all the net toroidal current flows and a ring in which flow Pfirsch-Schlüter currents given by (6) with $dI/d\phi = 0$.

In a straight geometry this would be stable to very high β. It is not so in a torus. Figure 4 shows the square of the growthrate of the most unstable n = 1 mode normalized to the time scale (1) as a function of the pressure,

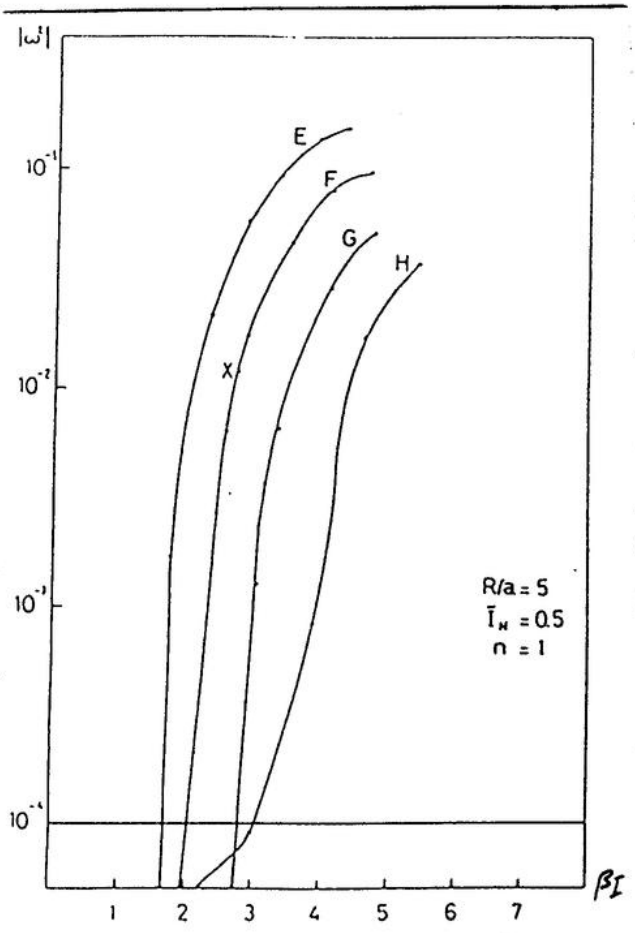

Fig. 4: The square of the growthrate of the n = 1 kink instability, normalized to the Alfvén transit time (1), as function of β_I for the four current and pressure profiles shown in Fig. 3. Calculation made with ERATO (Ref. 8).

measured by β_I (eq. 10), for the four equilibria EFGH of figure 3a. The threshold of significance is set at $|\omega^2| = 10^{-4}$. The problem of the discretizsation error and the reason for the choice of this value are discussed in ref. (12). A rapidly growing instability develops above a critical β_I. The threshold first increases as the current is concentrated deeper in the plasma (sequence E,F.G.H), namely as q_o is decreased. But when q_o drops below 1 (H), the forcefree internal kinks are further destabilized by the pressure and there is no stable range. This behaviour manifests itself in the H case by the break in the curve which is part of a pedestal just below 10^{-4} which extends to $\beta_I = 0$.

The displacement vector $\underline{\xi}$ in the particular meridian plane where the motion is up-down symmetric is shown in figure 5. It corresponds to the F equilibrium shown with a cross x in figure 4. The mode looks like a rigid m = 1 kink of the central current carrying region with a complicated pattern in the outer region where $p' \neq 0$. For this case $q_a = 3.688$ and $q_o = 1.19$. There are two singular surfaces q = 2 and 3 located in the outer region. If a Fourier expansion of the displacement vector in the poloidal angle θ is done on each ψ surface, it is seen that the dominant component is m = 1 in the core, becomes 2 around q = 2, 3 near q = 3 and m = 4 at the surface. This migration of the dominant poloidal mode index m to remain of the order of q is called «mode

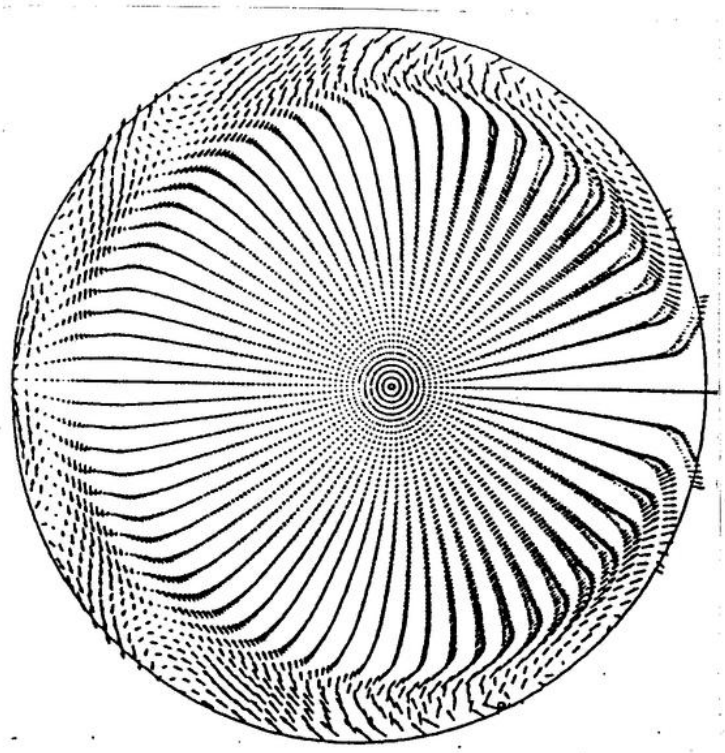

Fig. 5: The displacement vector of the pressure driven n = 1 instability of an F equilibrium at $\beta_I = 2.6$.

ballooning». It is a very important mechanism which couples a large number of ms.

For $n \neq 1$ the local m follows nq. Loosely speaking, the mode adapts its m to the local nq in order to extend radially. In the example shown this ballooning is clearly a destabilizing mechanism which leads to a maximum value of β_I, and thus of β. The trend is clear. It is best to have the current as peaked as possible compatible with the requirement that $q_o > 1$. It means in figure 1 to stay near the left edge of the stable range at $q_o > 1$. The pressure gradient progressively weakens the stabilizing influence of the net current free region and the n = m = 1 kink of the central region reappaers as if the plasma boundary were right on the core. Note that in the outer region there are large Pfirsch-Schlüter parallel currents which flow in opposite directions on the inside and outside of the torus with no net toroidal current (dipole distribution).

As n increases, the general behaviour is the same but the threshold moves to lower β_I. The stability limit for $n = \infty$ can be computed with the ballooning mode criterion described below. It is at $\beta_I = 1.2$ for the G equilibrium, much below the n = 1 limit. By moving the point where the pressure gradient vanishes towards the axis while keeping the location of the maximum at the same location until it is ballooning stable and enlarging simultaneously slightly the current channel to keep q_o from dropping below 1, it is possible to move the $n = \infty$ stability limit above the n = 1 limit. For the equilibrium G the final stable equilibrium has $\beta_I = 2.47$ or $\beta = 1.58\%$, only slightly less than the critical β_I shown in Fig. 4.

This example shows that the pressure destabilisation of the n = 1 kink does not have the same physical origin than ballooning instabilities since the n = 1 limit only feels the pressure and not its profile while the ballooning stability criterion is a local condition on the pressure gradient. We have not yet checked if for the final optimised equilibrium the low n > 1 modes are also stable.

8. THE BALLOONING CRITERION

In the limit $n \to \infty$ the most dangerous modes are localized radially, but they nevertheless extend through an ever increasing number of singular surfaces. This feature has been nicely shown in stability runs made with the PEST code /13/ and the theory has since been fully developed. The paper by J. Greene and M. Chance /14/ provides a good presentation of the problem as well as the motivitation for the recent attempts to overcome completely the β limit by shaping the plasma (access to the second stability region) /15/.

Since the most dangerous modes (the last ones to disappear and not the fastest growing!) are radially localized, stability must be checked surface by surface through the whole plasma. Near the axis it reduces to the well-known Mercier criterion /16/. It can be shown that the Mercier criterion on any magnetic surface is never more stringent than the ballooning criterion on this surface so that it does not need in principle to be verified independently. In practice, the ballooning criterion becomes very difficult to use near the axis while the Mercier criterion is very easy to use, so that this last criterion is a good substitute near the magnetic axis.

The ballooning criterion for the stability of the $n \to \infty$ modes can be written as $\mathrm{Min}\{\delta W_B(\phi)\} \geq 0$ on each surface, where $\delta W_B(\phi)$ can be written as /17/.

$$\delta W_B(\phi) = \int_{-\infty}^{+\infty} d\chi \left\{ \frac{T^2}{q^2 r^4 B_p^2} \left[1 + \left(\frac{r^2 B_p^2}{B} \nu \right)^2 \right] \left(\frac{\partial X}{\partial \chi} \right)^2 \right.$$

$$\left. - 2 \frac{r^2}{B^2} \mu_o^2 \frac{dp}{d\phi} \left[\frac{\partial}{\partial \phi} \left(p + \frac{B^2}{2\mu_o} \right) - \frac{T^2}{B^2 q r^2} \nu \frac{\partial}{\partial \chi} \left(\frac{B^2}{2\mu_o} \right) \right] X^2 \right\}. \qquad (14)$$

The variable of integration χ is a poloidal angle defined by

$$q\chi(\phi) \equiv \int_0^{\ell} d\ell \, \frac{T}{r^2 B_p}, \qquad (15)$$

the origin being chosen in the mid-plane, and

$$\nu(\psi) \equiv \frac{\partial}{\partial\psi}\left(q(\chi-\chi_o)\right). \qquad (16)$$

The angle $\chi_o(\psi)$ is a free parameter. The variable X upon which minimisation is done is related to the normal perturbation component ξ_n of the displacement. The extension of the range of integration in χ from one period to infinity is essential /17/. All coefficients are periodic except ν which goes asymptotically as χ. The ψ derivatives in (14) and (16) are taken along the normal to the magnetic surface. It is immediate from (14) that ballooning instabilities are driven by the pressure gradient.

It is known for some time that the ballooning criterion does not always limit the pressure gradient /15,18,19/. Take any force-free equilibrium, increase the pressure gradient $|p'|$ locally in a narrow region in ψ. An unstable band of $|p'|$ is first encountered which is sometimes followed by another stable region, called the second region of stability. As long as the pressure gradient is modified in this way in a sufficiently small region, the equilibrium is not much modified. It suggests that it should be possible to reach very high values of β ballooning stable. But the transition from localized modifications of the pressure and current gradients to a fully stable high β equilibrium is not so simple. As β increases, the overall equilibrium is affected, with an outward shift of the magnetic axis.

Attempts have been made to find high β equilibria everyhwere in the second stability region, or even better to find equilibria in which the unstable band between the two regions of stability disappears. Reference (15) is a good presentation of this approach which leads to strongly indented plasma cross-section (bean shape). The experiment PBX in Princeton has been built to test this concept.

There is no evidence so far that there is also a second stability region for the low-n modes, so that wall stabilisation of the low-n modes is an essential ingredient in this approach to high β operation.

8. A SCALING LAW FOR THE PRESSURE LIMIT

We have seen that pressure destabilizes the n = 1 free boundary modes and the high n modes (first region of stability). From the many parametric studies which have been published there are some general trends which emerge clearly:

As the pressure increases, the line in figure 1 which defines the stability limit on the right side swings back to the left and reduces the stable

range, in the same way as an increase in the current gradient at the edge. This is seen in all studies in which stability is studied by moving along constant q_a/q_o lines, by the appearance of new unstable regions for higher values of q_a and the progressive merging of the existing unstable bands (clear examples in ref. 9).

The left limit $q_o = 1$ is only affected by the pressure gradient in the central region. The Mercier criterion on axis may force q_o to increase slightly if the magnetic surfaces are non-circular. But the disappearance of the unstable region seems to occur mostly by the closing in of the right-hand stability boundary.

Here is a summary of extensive calculations made in Lausanne with ERATO to verify these trends, quantify the β limit and try to identify its dependence on the global parameters of the equilibrium. Details can be found in references 20-23.

The shape of the plasma surface is given by the three parameter formula

$$\begin{aligned} r &= R + a\cos(\theta + \gamma\sin\theta) \\ z &= E\,a\sin\theta, \end{aligned} \qquad -\pi \leq \theta < \pi \qquad (17)$$

where E is the elongation and γ the triangularity.

The profiles are specified by TT' and p'

$$\begin{aligned} TT' &= t\psi \\ p' &= p_1\psi + p_2\psi^2 \end{aligned} \qquad (18)$$

The three parameters t, p_1, p_2 allow to vary I, β and, in a certain range, q_o, but the q profile is not always monotonic. It assumes that there is no stabilizing shell or conductors around the plasma.

The choice of parameters has been governed by the necessity of relevance so that most of the work has been concentrated on the INTOR reference set of parameters and on JET, which have essentially the same shape, namely $E = 1.6 - 1.7$ and $\gamma = 0.3$.

The stability limits for JET in the plane (q_o, β), for a constant current of 4.8 MA, are shown in figure 6. Stability is down and to the right of the various curves. The n = 1 limit has the expected behaviour except for the slow drop with increasing q_o. The line labeled M is the Mercier limit on axis with stability on the right side. The line B is the limit under which all surfaces are ballooning stable. When it is crossed, high n instabilities first appear about half-way between the axis and the surface. The Mercier

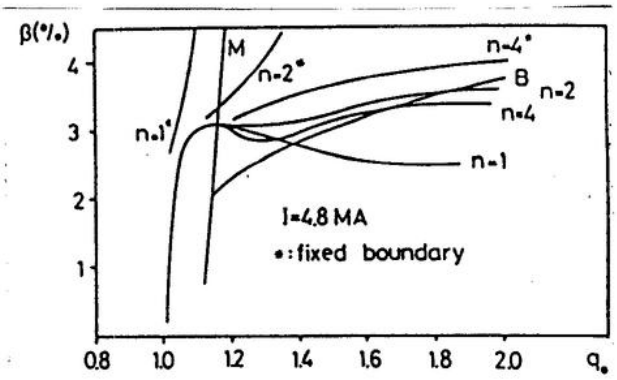

Fig. 6: The JET stability diagram. The limits labeled n = 1,2,4 are free boundary stability limits. M = Mercier limit on axis, B = ballooning limit.

line corresponds to high n unstable modes localized near the axis. It explains that the B line does not join smoothly with M. The limits for higher n are shown but they should be viewed with some caution because of the resolution which may be insufficient.

By tailoring locally the pressure profile it is possible to bring B above the top of the n = 1 limit so that, in this case also, the β limit seems to be set by the n = 1 mode. If one could accept B as the limit much higher β could be obtained. For q_o = 3.75 (hollow q profile!) the B limit is at 5%.

The calculation has been repeated for different currents, for different shapes and triangularities but, except for JET and INTOR, not in a systematic fashion, and the result is a β limit always set by the n = 1 free-boundary mode (stable to n = ∞ but not checked for intermediate ns). Figure 7 shows the n = 1 β limit obtained for various currents and three different aspect ratios with almost identical plasma shapes. The normalized current I_N is defined as

$$I_N \equiv \frac{\mu_o I}{aB} \qquad (19)$$

where B is the vacuum toroidal field in the centre of the plasma.

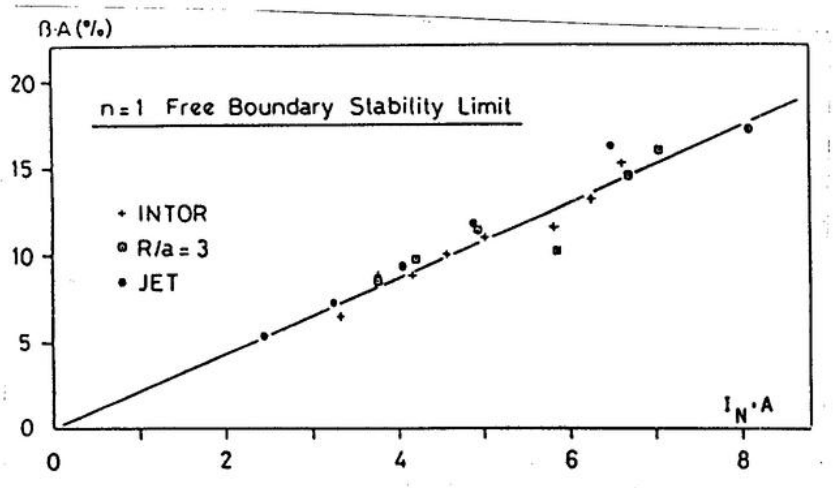

Fig. 7: Dependence of the n = 1 free boundary β limit on the normalized current I_N, for different aspect ratios A = R/a.

The simple formula

$$\beta(\%) = 2.2\, I_N \qquad (20)$$

is a good fit through all the points. The dependence of the limit on triangularity and elongation at a constant aspect ratio of 4 is shown in figure 8. The line (20) is also shown and the fit is equally good. The scatter of the points around the line is in part the result of the limited optimisation which has been done for the cases not relevant to JET or INTOR, but it must also reflect a residual dependence on other parameters, for example a reminiscence of the discontinuities seen at integer values of q_a in the $\beta = 0$, large aspect ratio stability diagram.

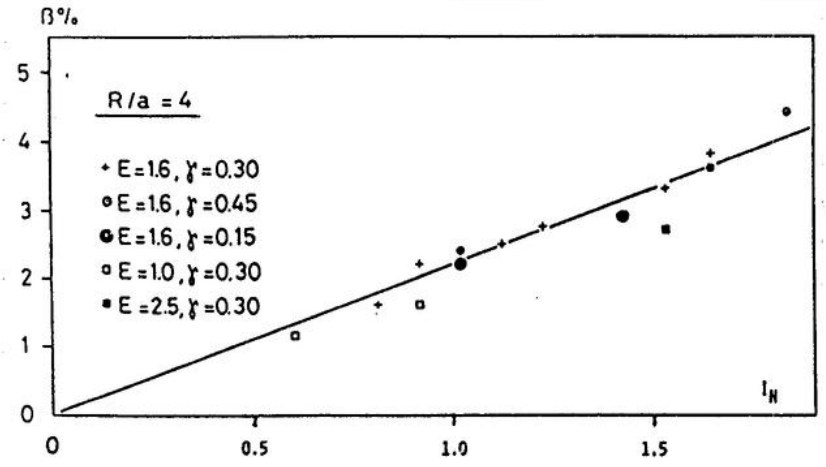

Fig. 8: Dependence of the n = 1 free boundary β limit on the normalized current I_N, for various shapes and the same aspect ratio A = 4.

The law (20) does not provide the ultimate limit until we know the limiting current.

In all the documented cases we know of, the limit on the current was near $q_a = 2$, also for JET in spite of its small aspect ratio and D shape. The law (20) seems to hold up to the maximum current.

The difficulty of calculating the stability of all configurations which have very high shear at the edge or an X-point as in divertored discharges may explain that the limit is always found at $q_a = 2$. It may mean that the shape has always been chosen such that shear is not too large at the edge. More numerical work is needed to clear this point, but experimental information with divertor discharges shows that there is still a current limitation and it is about where you expect it if you either "smooth" the surface to define an effective q or define q through the averaged current density /11/.

9. COMPARISON WITH EXPERIMENTAL DATA

The relation (20) has gained popularity when it was realized that it gave a good estimate of the highest β achieved in all the devices which have made a significant effort to increase β with strong auxiliary heating.

Figure 9 shows the result of a compilation made to see if a law such as (20) had any relevance to experiments /24/. It only used data published until the end of 1983. The agreement is surprising and additional results obtained since have not broken the limit in a decisive manner.

10. NON-UNIQUENESS OF THE LAW

There are alternative interpretations to the law (20). A. Sykes /25/ has shown by numerical calculations that the ballooning criterion leads to the same dependence if the q profile is assumed to increase regularly from $q_o = 1$ on axis to its value at the surface. Apparently, with his assumed q profile, shear is sufficient to provide a limit everywhere on the pressure gradient (no access to the second stability region). The difference is in the coefficient in front of the current in (20) which is 3.3.

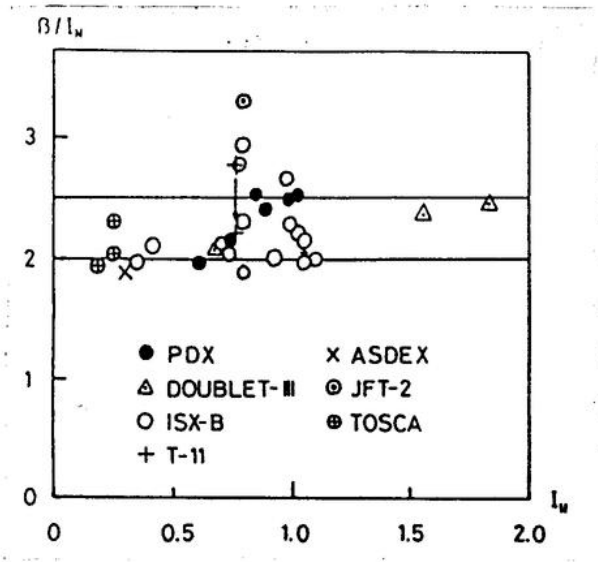

Fig. 9: Record discharges in the R, I_N plane. $R = \beta/I_N$. The values linked by an arrow are for identical discharges which have been analysed twice. The two horizontal lines at R = 2.0 and 2.5 delimited the range of maximum β found in the numerical computations (from Ref. 24).

In the calculations made which led to the relation (20), there was no wall stabilisation. It may very well be that, with a wall, tearing modes are also destablized by pressure by the same mechanism which destabilizes the n = 1 kink and that the law is really a tearing mode criterion.

11. AXISYMMETRIC INSTABILITIES

The n = 0 instabilities are positional instabilities. Their properties are well known /1/ and they are cured by a combination of passive and active stabilisation, the vacuum vessel and properly connected conductors close to the plasma providing the stabilisation on the fast time scale and an active feedback system providing the long term stability. There are no outstanding physics problems left to be solved comparable to that of the non-axisymmetric modes.

REFERENCES

/1/ BATEMAN, G., MHD Instabilities, The MIT Press (1980) 977.

/2/ GRIMM, R.C., et al., Methods of Computational Physics, Vol. 16, 253.

/3/ GRUBER, R., et al., Comp. Phys. Commun. 21 (1981) 323.

/4/ BERNARD, L.C., et al., Comp. Phys. Commun. 24 (1981) 373.

/5/ DEGTYAREV, L.M., et al., Proc. Int. Conf. on Plasma Physics, Lausanne, Switzerland, 1984, Vol. I, 157.

/6/ WESSON, J., Nucl. Fusion 18 (1978) 87.

/7/ SHAFRANOV, V.D., Sov. Physics - Techn. Phys. 15 (1970) 1751.

/8/ TURNBULL, A., TROYON, F., Post-deadline paper in the 12th European Conference on Controlled Fusion and Plasma Physics, Budapest, 1985.

/9/ KERNER, W., et al., Nucl. Fusion 23 (1981) 1383.

/10/ BUSSAC, M.N., et al., Phys. Rev. Letters 35 (1975) 1638.

/11/ OHYABU, N., et al., Nucl. Fusion 25 (1985) 49.

/12/ GRUBER, R., and RAPPAZ, J., Finite element methods in linear ideal magnetohydrodynamics, Springer 1985.

/13/ TODD, A.M.M., Phys. Rev. Letters 38 (1977) 826.

/14/ GREENE, J. and CHANCE, M., Nucl Fusion 21 (1981) 453.

/15/ GRIMM, R.C., et al., Nucl. Fusion 25 (1985) 805.

/16/ MERCIER, C., Nucl. Fusion Suppl. 2 (1962) 801.

/17/ TAYLOR, J.B. et al., Proc. Royal Soc. A. 365 (1978) 1.

/18/ MERCIER, C., Plasma Physics 21 (1979) 589.

/19/ COPPI, B., et al., Phys. Rev. Letters 44 (1980) 990.

/20/ SAURENMANN, H., et al., Plasma Physics and Controlled Nuclear Fusion Research, 1982 (Proc. 9th Int. Conf. Baltimore, 1982), Vol. 3, IAEA, Vienna (1983) 17.

/21/ TROYON, F., et al., Plasma Phys. and Contr. Fusion 26 1A (1984), 209.

/22/ INTOR, Phase IIA, European Contr. EUR FU BRU/XII-132/82/EDV30 (1982) 72.

/23/ SAURENMANN, H., et al., CRPP Laboratory Report, LRP 263/85 (1985).

/24/ TROYON, F. and GRUBER, R., Phys. Letters, 110A (1985) 29.

/25/ SYKES, A., et al., Contr. Fusion and Plasma Physics (Proc. 11th Europ. Conf., Aachen, 1983), European Physical Society (1983) B23.